Test for Arsenic Speciation in Waters based on a Paper-Based Analytical Device with Scanometric Detection

Francisco Pena-Pereira, Lorena Villar-Blanco, Isela Lavilla, Carlos Bendicho*

Analytical and Food Chemistry Department; Faculty of Chemistry; University of Vigo, Campus As Lagoas-Marcosende s/n, 36310 Vigo, Spain

Tel.: +34 986812281; fax: +34 986812556; e-mail address: bendicho@uvigo.es

Highlights:

- A low-cost non-instrumental method for As speciation analysis is proposed.
- The method involves three phase microseparation with colorimetric reaction at the PAD's detection area.
- The physical separation of detection and injection zones avoids chemical incompatibility.
- The method enables determination of As(III), As(V) and total inorganic As in waters.
- The assay can be applied as a vanguard analytical system for total As screening.

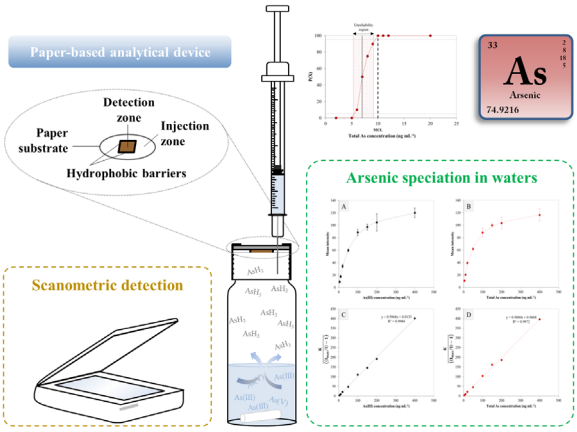

Graphical abstract

Test for Arsenic Speciation in Waters based on a Paper-Based Analytical Device with Scanometric Detection

Francisco Pena-Pereira, Lorena Villar-Blanco, Isela Lavilla, Carlos Bendicho*

Analytical and Food Chemistry Department; Faculty of Chemistry; University of Vigo, Campus As Lagoas-Marcosende s/n, 36310 Vigo, Spain

Tel.: +34 986812281; fax: +34 986812556; e-mail address: bendicho@uvigo.es

Abstract

A rapid, simple and affordable method for arsenic speciation analysis is described in this work. The proposed methodology involves *in situ* arsine generation, transfer of the volatile to the headspace and its reaction with silver nitrate at the detection zone of a paper-based analytical device (PAD). Thus, silver nitrate acts as a recognition element for arsine in the paper-based sensor. The chemical reaction between the recognition element and the analyte derivative results in the formation of a colored product which can be detected by scanning the detection zone and data treatment with an image processing and analysis program. Detection and injection zones were defined in the paper substrate by formation of hydrophobic barriers, thus enabling the formation of the volatile derivative without affecting the chemical stability of the recognition element present in the PAD. Experimental parameters influencing the analytical performance of the methodology, namely color mode detection, composition of the paper-based sensor and hydride generation and mass transfer conditions, were evaluated. Under optimal conditions, the proposed method showed limits of detection and quantification of 1.1

and 3.6 ng mL^{-1}, respectively. Remarkably, the limit of detection of the method reported herein was much lower than the maximum contaminant levels set by both the World Health Organization and the US Environmental Protection Agency for arsenic in drinking water, unlike several commercially available arsenic test kits. The repeatability, expressed as relative standard deviation, was found to be 7.1% (n=8). The method was validated against the European Reference Material ERM®-CA615 groundwater and successfully applied to the determination of As(III), As(V) and total inorganic As in different water samples. Furthermore, the method can be used for the screening analysis of total arsenic in waters when a cut-off level of 7 ng mL^{-1} is used.

Keywords

Paper-based analytical device; arsenic speciation; non-instrumental detection; scanometric analysis; screening; water analysis

1. Introduction

Groundwater contamination with arsenic has become a major global issue. Millions of people worldwide are exposed to this pollutant at concentrations above current drinking water standards. The situation is especially worrisome in Bangladesh, where 35-77 million people have been estimated to be chronically exposed to arsenic contaminated drinking water [1]. Although the maximum contaminant level (MCL) for this pollutant in drinking water has been set at 10 ng mL^{-1} by both the US Environmental Protection Agency (USEPA) and the World Health Organization (WHO), many developing countries still retain a 50 ng mL^{-1} standard. Remarkably, more stringent and challenging drinking water standards are expected to be set for arsenic in the future [2–4]. Thus, the development of rapid, cost-effective and sensitive analytical methodologies for arsenic

monitoring in drinking water samples that meet with current and future standards for arsenic is of paramount importance.

Arsenic is predominantly present in the form of inorganic species in water samples, namely As(III) and As(V), whereas organic arsenic species such as methylarsonic acid, dimethylarsinic acid or trimethylarsine oxide are not considered of quantitative importance in waters [3,5]. The determination of arsenic species rather than the total content is highly desirable bearing in mind that they significantly differ in toxicity. Chromatographic techniques coupled with elemental detection systems are typically employed for arsenic speciation [6–8]. Alternatively, non-chromatographic methodologies, including electrochemical methods [9,10] or the combination of spectrometric detection techniques such as atomic absorption spectrometry [11–13], atomic fluorescence spectrometry [14], inductively coupled plasma mass spectrometry [15] or UV-vis spectrophotometry [16,17] with selective extraction of arsenic species [11,12,15] or hydride generation [14,16,17] have also been reported in the literature [3,18].

Since their inception in 2007 [19], the development and application of paper-based analytical devices (PADs) has undergone a continuous growth due to their simplicity, low-cost, portability and feasibility for the non-instrumental analysis by means of everyday communications and information technology (IT) equipment [20,21]. The applicability of PADs in the analysis of biomedical, food, and environmental samples has been extensively demonstrated [22–25]. However, the reduced sensitivity of PADs usually hinders their applicability to the monitoring of target analytes present at trace and ultratrace levels. With the aim of overcoming this drawback, a number of preconcentration approaches have been reported in the literature, most of them being applicable to the enrichment of non-volatile compounds [26–31]. It is noteworthy,

however, that the number of reports devoted to monitoring volatile analytes or derivatives by using PADs is yet scarce, and the limits of detection (LODs) achieved with them are within the ppm level when preconcentration is not involved [31–33]. This fact represents a serious hindrance in monitoring environmentally relevant volatile analytes or derivatives by means of PADs. An appealing approach involving the headspace solid phase extraction of *in situ* generated H_2Se by a quantum dots-based PAD has been recently reported for determination of selenium in urine samples on the basis of fluorescence quenching, providing an advantageous PAD with improved sensitivity and selectivity [31]. However, the recognition element used in the reported PAD covered the whole area of the paper substrate, so a lack of chemical compatibility of the recognition element with the chemicals involved in the *in situ* generation of volatiles could restrict or even prevent the applicability of the PAD in alternative analytical systems.

The main aim of this work involves the development of a novel PAD for speciation analysis of arsenic in water samples. The method relies on the microreaction of arsine generated *in situ* with silver nitrate at the detection zone of a paper substrate and subsequent scanometric analysis of the colored product. Formation of hydrophobic barriers in the paper substrate is proposed herein to physically separate detection and injection zones in the PAD, thus overcoming the reduction of silver ions produced by injection of sodium borohydride solution through the substrate. The possibility of carrying out speciation analysis with the reported PAD was assessed by carefully controlling the hydride generation conditions.

2. Experimental

2.1.Reagents and materials

All chemicals were of analytical reagent grade. High-purity deionized water was produced from a PETLAB ultrapure water system (Peter Taboada, Vigo, Spain). Stock solutions of As(III) and As(V) were prepared from As_2O_3 and As_2O_5 (Merck, Darmstadt, Germany), respectively. Working standard solutions were prepared daily by appropriate dilution of the stock solutions. $AgNO_3$ (Riedel-de Haën, Seelze, Germany) was used as recognition element. Hydrochloric acid (Prolabo), citric acid monohydrate (Sigma-Aldrich, St. Louis, MO, USA), and $NaBH_4$ (Merck) stabilized with 0.1 mol L^{-1} NaOH (Prolabo, Paris, France) were used for hydride generation. The following reagents were used for evaluation of potential interferences: K_2HPO_4, $Pb(NO_3)_2$, $Ni(NO_3)_2.6H_2O$, $NaNO_2$, $Na_2S.9H_2O$ and H_2SeO_3 (Panreac, Barcelona, Spain), $CuSO_4.5H_2O$ (Probus, Badalona, Spain), NaCl and $Bi_5O(OH)_9(NO_3)_4$ (Merck), $NaHCO_3$, Na_2SO_4 and $SbCl_3$ (Carlo Erba, Milan, Italy), Na_2TeO_3 (Sigma-Aldrich) and humic acid (Fluka Chemie, Buchs, Switzerland).

Whatman No. 1 (180 µm, 87 g m^{-2}) and Whatman No. 3 (390 µm, 185 g m^{-2}) filter papers obtained from Whatman (Maidstone, Kent, UK) were assessed as paper substrates. A Lumocolor permanent pen 318-9 fine 0.6 mm (Staedtler, Nuremberg, Germany) was used to prepare the hydrophobic barriers on paper substrates.

Microextraction experiments were carried out by using 40 mL-amber vials sealed with screw top hole caps with PTFE faced-septa.

An HP 4500 desktop scanner was used to digitize PADs after microextraction experiments. Alternative systems such as digital cameras, cell phones or smartphones could also be used for quantitative readout as reported in the literature [22].

2.2.Characterization of PADs

A JEOL JSM 6700 FEG-SEM scanning electron microscope equipped with an Oxford Inca Energy 300 energy-dispersive X-ray spectrometer (EDS) was used for characterization of PADs. SEM images were obtained with an acceleration voltage of 10 kV using backscattered electron detection. EDS spectra were obtained at 15 kV.

2.3.Preparation of PADs

First, Whatman No. 3 filter papers were cut into circular pieces of 20 mm diameter. Then, PADs were prepared following previously reported fabrication processes [34,35]. Accordingly, hydrophobic barriers with a square side length of 8 mm were drawn on the upper side of the paper substrate with a permanent marker to define the detection area and, after the ink solvent was evaporated, the process was repeated on the lower side of the paper substrate. Once the ink solvent was evaporated, 10 µL of $AgNO_3$ solution was spotted in the detection zone and the prepared PAD was allowed to air-dry protected from the light and stored at 4ºC into a zipper bag until analysis.

2.4.*Experimental procedure and data analysis*

A schematic representation of the system used for arsenic sensing is shown in **Fig. 1**. A circular PAD prepared according to the procedure described in section 2.3 was placed inside a screw top hole cap over a PTFE-faced septum. The recognition element (silver nitrate) for arsine was thus exposed to the headspace above the sample for analysis. Selective determination of As(III) was carried out by placing a 5 mL solution containing citric acid 0.5% (m/v) into a 40 mL amber vial. Alternatively, a 5 mL solution in HCl 1 mol L^{-1} was placed into a 40 mL amber vial for total inorganic As determination. Arsine generation was carried out in both cases by externally injecting 1 mL of 1% (m/v)

$NaBH_4$ though the injection zone of the PAD to those solutions stirred at 900 rpm for 5 min. The concentration of As(V) was determined by mathematically subtracting the concentration of As(III) from the concentration of total inorganic As. In the presence of arsenic, a colored product was obtained in the modified paper substrate as a result of the reaction between the evolved arsine and the silver-containing PAD. The detection zone of PADs was then digitized by means of a desktop scanner. Quantification was carried out by using Image J, a free image processing and analysis software [36]. Images were imported into Image J, inverted, and the mean color intensity was quantified using the red channel at the RGB color space.

3. Results and discussion

3.1.Evaluation of experimental parameters

A number of experimental parameters that can influence the analytical performance of the proposed test were evaluated, including the color mode detection, the composition of the paper-based sensor and the arsine generation and mass transfer conditions.

3.1.1. Color mode detection

The effect of the color mode detection conditions on the analytical signal was initially evaluated by subjecting a 100 ng mL^{-1} As(III) solution to the microextraction procedure. The $AgNO_3$-containing PAD was subsequently digitized and processed by using ImageJ. The image was thus converted into grayscale (GS), RGB and MCYK color modes, and the mean color intensities of both blanks and standards are shown in **Fig. 2**. It can be observed from the figure that the different color modes yielded similar corrected analytical responses. Nevertheless, the red channel provided the lowest intensity for blanks and, therefore, better signal-to-noise ratios. Consequently, the red

channel was selected for subsequent studies since it yielded acceptable sensitivity for AsH_3 detection with considerably lower blank values.

3.1.2. Composition of the paper-based sensor

The type of filter paper used as substrate to prepare the PAD for arsenic detection was also evaluated. PADs were prepared using two different substrates, namely Whatman No. 1 and Whatman No. 3 filter papers. The analytical response obtained with Whatman No. 1 was ca. 23% higher than obtained with Whatman No. 3, presumably due to its reduced thickness and porosity. However, Whatman No. 3 yielded ca. 45% lower blanks than Whatman No. 1. Thus, Whatman No. 3 filter paper was finally selected for further experiments since it gave rise to better signal-to-noise ratios for arsenic detection.

The amount of the recognition element ($AgNO_3$) present in the detection zone of the PAD was subsequently evaluated in the range 0.1-5.0 mg, and the obtained results shown in **Fig. 3**. As can be observed from the figure, the mean color intensity sharply increased with increasing the mass of $AgNO_3$ up to 1 mg, and thereafter a less pronounced decrease of the analytical response was observed. According to the obtained results, a mass of 1 mg $AgNO_3$ was selected as it provided a high sensitivity with reduced reagent consumption.

3.1.3. Arsine generation and mass transfer conditions

Hydride generation conditions were assessed for optimal performance. The effect of sodium borohydride concentration on the analytical response was firstly studied. **Fig. 4A** shows that the analytical response almost linearly increased when the concentration of the reducing agent was increased in the range 0.25-1% (m/v). A further increase in

the concentration of $NaBH_4$ resulted in a slight decrease of the analytical signal presumably due to the increasing amounts of hydrogen produced under these conditions [37]. Consequently, the reducing agent concentration was set at 1% (m/v) for further investigations.

The possibility of selectively determine inorganic arsenic species by careful control of the reaction medium conditions was subsequently evaluated. It has been reported in the literature that the acidity of the aqueous solution plays a paramount role in the selective generation of hydrides from arsenic species. Specifically, the reduction of individual arsenic species with $NaBH_4$ is dependent on the pK_a of the individual arsenic acids and, therefore, AsH_3 can be selectively generated from inorganic arsenic species by controlling the pH of the reaction media. Both inorganic arsenic species are reduced to arsine in strong acid environment, whereas the use of weak organic acids such as citric acid can hamper the formation of arsine from As(V) [13]. Thus, we evaluated the effect of the concentration of hydrochloric acid and citric acid on the generation of arsine from As(III) and As(V). The obtained results are displayed in **Figs. 4B** and **4C**. As can be observed from **Fig. 4B**, the analytical signal of As(V) sharply increased by increasing the concentration of HCl in the range 0.01-0.5 mol L^{-1} and remained constant above this concentration, whereas the maximum analytical response for As(III) was achieved when an HCl concentration above 0.1 mol L^{-1} was used. The analytical responses were similar irrespective of the arsenic species when the HCl concentration was set in the range 1-2 mol L^{-1}, so an HCl concentration of 1 mol L^{-1} was finally chosen to determine total inorganic As. The effect of the concentration of citric acid on the analytical response of As(III) and As(V) was then assessed. As can be observed (**Fig. 4C**), the analytical signal corresponding to As(V) significantly decreased when citric acid concentrations below 5% (m/v) were used, showing a negligible response

when the citric acid concentration was set at 0.5% (m/v). On the contrary, the analytical response of As(III) was almost constant in the range 0.5-30% (m/v). According to these results, a citric acid concentration of 0.5% (m/v) was selected for selectively determining As(III).

The sampling time was finally evaluated, bearing in mind that the mass transfer process involved is time-dependent. As can be seen in **Fig. 5**, the analytical signal significantly increased with increasing the sampling time up to 3 min and reached a plateau in the range of 5-20 min. Accordingly, a 5 min time was selected as the optimum since it enabled excellent sensitivity and acceptable sample throughput.

3.2.Evaluation of the thermal stability of PADs

It has been reported in the literature that Ag(I) ions could be reduced to Ag^0 due to the reducing groups (hemiacetal and alcoholic groups) of cellulose, and the formed Ag^0 could catalyze further reduction of Ag(I). In addition, the reduction process can be favored by factors such as high temperature, presence of light an alkaline pH [38]. With the aim of assessing the practical applicability of PADs for AsH_3 sensing, we have evaluated the stability of PADs at three different storage temperature conditions, namely 20 ºC, 4ºC and -20ºC during a 20-day period. In all cases, PADs were kept protected from light to avoid the well-known photo-induced reduction of Ag(I) ions [39,40]. As expected from the above, the stability of PADs was found to be clearly dependent on the storage temperature. PADs stored at -20 ºC were found to be very stable in the whole evaluated storage time. Specifically, blank values were not significantly increased in the whole evaluated period, and the analytical response of As(III) was practically not affected in the evaluated range, showing a 10% decrease from its initial value after being stored at -20ºC for 20 days. Oppositely, the mean color intensity of

PADs stored at room temperature increased with increasing the storage time and, thus, blank values significantly worsen (mean color intensity > 10) after two hours of storage. Moreover, the sensitivity achieved with PADs stored at room temperature significantly decreased after 1 day of storage, being reduced in ca. 70% of its initial value after a 20-day period. PADs stored at 4ºC showed an intermediate behavior, yielding a slightly higher stability than obtained at room temperature. Thus, blank values increased significantly (mean color intensity > 10) after 24 h, and were found to be better than obtained at room temperature during the first week. However, the analytical response decreased significantly in the whole studied range, even though the decrease was less pronounced than observed at room temperature.

It should be highlighted that no significant differences were observed between the corrected mean intensities obtained with PADs stored under the three evaluated temperature conditions during an 8h period, even though worse blank values were achieved after 2h of storage at room temperature. Thus, recently prepared PADs stored at room temperature or, preferably, refrigerator can be used for short term analysis, whereas the storage of PADs at -20 ºC is mandatory whether devices are not intended to be used immediately.

3.3.Analytical performance

Under optimal conditions, the analytical characteristics of the proposed method were obtained for As(III) and total inorganic As determination. **Figs. 6A** and **6B** show the relationship between the analytical response (mean color intensity) and the concentration of the target species. As expected from previous works involving colorimetric PADs [35,41], non-linear intensity *vs* concentration curves were observed for both As(III) and total inorganic As determination. Both curves, nevertheless,

showed a good agreement when adjusted to rectangular hyperbolic curves (**Figs. 6C** and **6D**). The corresponding rectangular hyperbolic equations, which relate the analytical response with the concentration of the target species, were rearranged for quantification purposes as described elsewhere [35]. Briefly, a linear relationship with theoretical unity slope and zero intercept was found between $K/((I_{max}/I)-1)$ and the analyte concentration, where I is the color intensity, I_{max} is the maximum achievable mean color intensity, and K is the concentration of the analyte corresponding to half of the I_{max}. The values of I_{max} and K were obtained for As(III) and total inorganic As determination using the Excel's Solver tool (Microsoft 2010). The values of I_{max} and K for As(III) determination were 139.0 and 62.9 ng mL^{-1}, respectively, whereas the corresponding I_{max} and K values for total inorganic As determination were found to be 131.5 and 51.4 ng mL^{-1}, respectively. The LOD, calculated at a signal-to-noise ratio of 3, was found to be 1.1 ng mL^{-1}, whereas the limit of quantification (LOQ), calculated at a signal-to-noise ratio of 10, was 3.6 ng mL^{-1}. The repeatability of the methodology, expressed as relative standard deviation (RSD), was 7.1% (n=8).

A comparison of the analytical figures of merit of the proposed methodology with alternative methods is provided in **Table 1**. As can be inferred from the data included in the table, the proposed method showed excellent sensitivity, acceptable repeatability, reduced sample consumption and high sample throughput. Remarkably, the low LOD achieved by the proposed methodology enabled the determination of inorganic As species in water samples at concentration levels below the MCL set by the USEPA and WHO for As in drinking water. When compared with commercial colorimetric and luminescent kits, the proposed method showed better LODs with reduced sample consumption and analysis time [42–46]. Moreover, the LOD of the proposed method was comparable or better than that obtained with recently reported

methods for total inorganic As determination based on the reaction of arsine with $HgBr_2$ or $AuCl_3$ [47–49], as well as for determination of arsenite on the basis of its interaction with nanoparticles-containing paper-based microfluidic devices [50,51].

3.4.Evaluation of interferences

The tolerance of the proposed method to a variety of potential interferences, namely transition metals, hydride generation elements, salts and humic acid, was assessed. Interference effects were considered when a variation of the analytical response beyond ±10% was observed in the presence of potential interferences. Transition metals did not yield any positive or negative effect on the analytical signal when present at concentration levels of 100 mg L^{-1} Pb(II), 2 mg L^{-1} Ni(II), 1 mg L^{-1} Cu(II), and 200 ng mL^{-1} Ag(I). Hydride forming-elements did not result in interferent effects when present at 25 mg L^{-1} Te(IV), 10 mg L^{-1} Se(IV), and 1 ng mL^{-1} Bi(III) and Sb(III). Regarding salts, 180,000 mg L^{-1} chloride, 30,000 mg L^{-1} carbonate and sulfate, 20,000 mg L^{-1} phosphate, 1,000 mg L^{-1} nitrite, and 10 mg L^{-1} sulfide did not cause any significant effect on the analytical signal. Furthermore, the proposed method was not affected by the presence of at least 25 mg L^{-1} humic acid.

3.5.Analysis of water samples

The proposed method was applied to the determination of As(III), As(V) and total inorganic As in four water samples with different complexity, namely bottled drinking water, river water, fountain water and seawater. As can be shown in **Table 2**, the concentration of arsenic species in the analyzed samples was found to be below the LOD of the reported method. Recovery studies were thus carried out by spiking water samples with As(III) and As(V) at different concentrations to assess the accuracy of the

method. The results obtained in the recovery studies are shown in **Table 2**. Recoveries in the range 88-112% were obtained for the inorganic As species considered, thus showing that the matrix of the different aqueous samples yielded negligible effects on the analytical response.

Furthermore, the method was validated against the European Reference Material ERM®-CA615 groundwater (certified concentration of total As: 9.9±0.7 ng mL^{-1}). No significant differences occurred between the found content (10.2±0.9 ng mL^{-1}) and the certified concentration since the experimental t value was lower than the critical t value (p=0.05).

3.6.Reliability of the screening methodology for total inorganic As monitoring

Finally, the feasibility of the proposed methodology as a sample screening method for total inorganic As determination was evaluated. Avoiding false negatives is of paramount importance in field screening test methods, since samples classified as negative are not re-tested. The unreliability of the screening methodology was assessed by constructing a probability-concentration graph (% positive results *vs* analyte concentration level) by setting a cut-off value close to the MCL set for total inorganic As in water samples [52]. As can be deduced from **Fig. 7**, a 7 ng mL^{-1} concentration level can be selected as a suitable cut-off level since the upper limit of the unreliability region (9.2 ng mL^{-1} of As) was below the allowable MCL for As (10 ng mL^{-1}). The screening method could therefore be used as a vanguard analytical system for total As assessment, and a confirmative (rearguard) analytical system such as hydride generation-atomic absorption spectrometry could be used for testing positive and inconclusive results [53].

3.7. Characterization of PADs and sensing reaction of AsH_3

PADs in the absence and presence of increasing concentrations of AsH_3 were characterized by SEM-EDS. It can be observed from the SEM images (**Fig. 8A-E)** that the exposure of silver-containing PADs to AsH_3 resulted in the formation of nanoparticles and larger size particles on the surface of cellulose microfibrils. Particularly, the exposure of Ag(I)-containing PADs to increasing amounts of AsH_3 resulted in an increasing density of quasispherical nanoparticles evenly distributed at the surface of cellulose microfibrils (as shown in the insets of **Fig. 8B-E**). The average diameter sizes of nanoparticles increased from c.a. 23 to 37 nm with increasing the concentration of AsH_3. Furthermore, larger particles were also formed at the surface of cellulose fibers, showing irregular shapes and a high size polydispersity. The size of particles slightly increased with increasing the initial As(III) concentration present in the sample, showing median sizes of up to ca. 365 nm for PADs exposed to AsH_3 generated from 400 ng/mL As(III). The EDS spectrum of a PAD exposed to AsH_3 generated from a 400 ng/mL As(III) solution (**Fig. 8F**) clearly shows As in its composition, thus confirming the chemisorption of AsH_3 at the PAD's detection area.

In summary, the proposed test involves arsine generation and its subsequent reaction with Ag(I) ions at the PAD's detection zone. The method firstly involves the *in situ* generation of volatile arsine (1):

$$H_3AsO_3 + 2BH_4^- + 2H^+ \rightarrow 2AsH_3 + 2H_3BO_3 + 3H_2 \quad (1)$$

Arsine generation occurs through a series of chemical reactions, namely formation of arsenic-borane complex intermediates, followed by internal hydrogen-transfer from boron to arsenic and fast hydrolysis of the intermediates, as reported by D'Ulivo et al. [54]. Ag(I) ions present at the PADs' detection area are presumably anchored onto cellulose fibers by ion-dipole interactions with the ether oxygen and hydroxyl groups

[38,55]. The evolved arsine can then react with excess $AgNO_3$ present at the PAD to form the double compound $Ag_3As.3AgNO_3$ (2), which in the presence of water could be decomposed to form Ag^0 (3) [56]:

$$AsH_3 + 6AgNO_3 \rightarrow AsAg_3.3AgNO_3 + 3HNO_3 \quad (2)$$

$$AsAg_3.3AgNO_3 + 3H_2O \rightarrow H_3AsO_3 + 6Ag^0 + 3HNO_3 \quad (3)$$

Moreover, the formed Ag^0 could catalyze the reduction of excess Ag(I) ions present at the PAD and, due to the absence of stabilizing agents, aggregation of Ag^0 clusters formed could led to the formation of larger particles [38,55].

4. Conclusions

This work reports on the development and application of a rapid and low-cost non-instrumental methodology for inorganic As speciation analysis. The method relies on the *in situ* generation of AsH_3 and chemical reaction of the hydride at the surface of a $AgNO_3$-containing paper substrate. The combination of a three phase microseparation approach with an integrated PAD containing the recognition element resulted in an efficient approach that enabled the quantitative determination of As species at concentration levels below the MCL set by both the WHO and USEPA, respectively. Under optimal conditions, the method was successfully applied to the determination of As(III), As(V) and total As in different water samples by exploiting the different reduction rate of inorganic As species in different acid reaction media. The method can also be applied to the rapid screening of total As in waters when a cut-off level of 7 ng mL^{-1} is used. Remarkably, the proposed methodology showed excellent sensitivity and sample throughput with a reduced sample consumption when compared with commercially available colorimetric kits for As determination. Besides, other everyday

communications and IT equipment such as mobile phones and digital cameras could also be implemented, thus expanding the applicability of the method.

Acknowledgements

Financial support from the Spanish Ministry of Economy and Competitiveness (Project CTQ2015-68146-P) (MINECO/FEDER) is gratefully acknowledged. F. Pena-Pereira thanks Xunta de Galicia for financial support as a post-doctoral researcher of the I2C program. The CACTI facilities (University of Vigo) are also acknowledged for obtaining SEM images and EDS analyses of PADs.

References

[1] M. Argos, T. Kalra, P.J. Rathouz, Y. Chen, B. Pierce, F. Parvez, et al., Arsenic exposure from drinking water, and all-cause and chronic-disease mortalities in Bangladesh (HEALS): A prospective cohort study, Lancet. 376 (2010) 252–258.

[2] A.A. Meharg, A. Raab, Getting to the bottom of arsenic standards and guidelines, Environ. Sci. Technol. 44 (2010) 4395–4399.

[3] J. Ma, M.K. Sengupta, D. Yuan, P.K. Dasgupta, Speciation and detection of arsenic in aqueous samples: A review of recent progress in non-atomic spectrometric methods, Anal. Chim. Acta. 831 (2014) 1–23.

[4] K. Henke, Arsenic: Environmental chemistry, health threats and waste treatment, John Wiley & Sons, Chichester, UK, 2009.

[5] W.H. Organization, World Health Organization, United Nations Synthesis Report on Arsenic in Drinking Water, (2001). http://www.bvsde.paho.org/bvsacd/who/arsin.pdf (accessed September 9, 2017).

[6] I. Komorowicz, D. Barałkiewicz, Arsenic speciation in water by high-performance liquid chromatography/ inductively coupled plasma mass spectrometry-method validation and uncertainty estimation, Rapid Commun. Mass Spectrom. 28 (2014) 159–168.

[7] J. Gorny, D. Dumoulin, L. Lesven, C. Noiriel, B. Madé, G. Billon, Development and application of a HPIC-ICP-MS method for the redox arsenic speciation in river sediment pore waters, J. Anal. At. Spectrom. 30 (2015) 1562–1570.

[8] I. Komorowicz, D. Barałkiewicz, Arsenic and its speciation in water samples by high performance liquid chromatography inductively coupled plasma mass spectrometry - Last decade review, Talanta. 84 (2011) 247–261.

[9] M. Yang, X. Chen, T.J. Jiang, Z. Guo, J.H. Liu, X.J. Huang, Electrochemical detection of trace arsenic(III) by nanocomposite of nanorod-like α-MnO2 decorated with 5 nm Au nanoparticles: Considering the change of arsenic speciation, Anal. Chem. 88 (2016) 9720–9728.

[10] D. Jedryczko, P. Pohl, M. Welna, Inorganic arsenic speciation in natural mineral drinking waters by flow-through anodic stripping chronopotentiometry, Talanta. 150 (2016) 265–271.

[11] V.G. Mihucz, L. Bencs, K. Koncz, E. Tatár, T. Weiszburg, G. Záray, Fast arsenic speciation in water by on-site solid phase extraction and high-resolution continuum source graphite furnace atomic absorption spectrometry, Spectrochim. Acta Part B At. Spectrosc. 128 (2017) 30–35.

[12] M. Shamsipur, N. Fattahi, Y. Assadi, M. Sadeghi, K. Sharafi, Speciation of As(III) and As(V) in water samples by graphite furnace atomic absorption spectrometry after solid phase extraction combined with dispersive liquid-liquid microextraction based on the solidification of floating organic drop, Talanta. 130

(2014) 26–32.

[13] H.M. Anawar, Arsenic speciation in environmental samples by hydride generation and electrothermal atomic absorption spectrometry, Talanta. 88 (2012) 30–42.

[14] S. Musil, T. Matoušek, J.M. Currier, M. Stýblo, J. Dědina, Speciation analysis of arsenic by selective hydride generation-cryotrapping-atomic fluorescence spectrometry with flame-in-gas-shield atomizer: Achieving extremely low detection limits with inexpensive instrumentation, Anal. Chem. 86 (2014) 10422–10428.

[15] C. Huang, W. Xie, X. Li, J. Zhang, Speciation of inorganic arsenic in environmental waters using magnetic solid phase extraction and preconcentration followed by ICP-MS, Microchim. Acta. 173 (2011) 165–172.

[16] K. Toda, T. Ohba, M. Takaki, S. Karthikeyan, S. Hirata, P.K. Dasgupta, Speciation-capable field instrument for the measurement of arsenite and arsenate in water, Anal. Chem. 77 (2005) 4765–4773.

[17] W. Boonjob, M. Miró, S.D. Kolev, On-line speciation analysis of inorganic arsenic in complex environmental aqueous samples by pervaporation sequential injection analysis, Talanta. 117 (2013) 8–13.

[18] A. Gonzalvez, M.L. Cervera, S. Armenta, M. de la Guardia, A review of non-chromatographic methods for speciation analysis, Anal. Chim. Acta. 636 (2009) 129–157.

[19] A.W. Martinez, S.T. Phillips, M.J. Butte, G.M. Whitesides, Patterned paper as a platform for inexpensive, low-volume, portable bioassays, Angew. Chemie - Int. Ed. 46 (2007) 1318–1320.

[20] L.F. Capitán-Vallvey, N. López-Ruiz, A. Martínez-Olmos, M.M. Erenas, A.J.

Palma, Recent developments in computer vision-based analytical chemistry: A tutorial review, Anal. Chim. Acta. 899 (2015) 23–56.

[21] K. Grudpan, S.D. Kolev, S. Lapanantnopakhun, I.D. McKelvie, W. Wongwilai, Applications of everyday IT and communications devices in modern analytical chemistry: A review, Talanta. 136 (2015) 84–94.

[22] D.M. Cate, J.A. Adkins, J. Mettakoonpitak, C.S. Henry, Recent developments in paper-based microfluidic devices, Anal. Chem. 87 (2015) 19–41.

[23] N. Meredith, C. Quinn, D. Cate, T. Reilly, J. Volckens, C. Henry, Paper-based analytical devices for environmental analysis, Analyst. 141 (2016) 1874–1887.

[24] Y. Yang, E. Noviana, M.P. Nguyen, B.J. Geiss, D.S. Dandy, C.S. Henry, Paper-based microfluidic devices: Emerging themes and applications, Anal. Chem. 89 (2017) 71–91.

[25] A.M. López-Marzo, A. Merkoçi, Paper-based sensors and assays: a success of the engineering design and the convergence of knowledge areas, Lab. Chip. 16 (2016) 3150–3176.

[26] A. Abbas, A. Brimer, J.M. Slocik, L. Tian, R.R. Naik, S. Singamaneni, Multifunctional analytical platform on a paper strip: Separation, preconcentration, and subattomolar detection, Anal. Chem. 85 (2013) 3977–3983.

[27] S.Y. Wong, M. Cabodi, J. Rolland, C.M. Klapperich, Evaporative concentration on a paper-based device to concentrate analytes in a biological fluid, Anal. Chem. 86 (2014) 11981–11985.

[28] X. Yuan, L. Renaud, M.C. Audry, P. Kleimann, Electrokinetic biomolecule preconcentration using xurography-based micro-nano-micro fluidic devices, Anal. Chem. 87 (2015) 8695–8701.

[29] S.-H. Yeh, K.-H. Chou, R.-J. Yang, Sample pre-concentration with high enrichment factors at a fixed location in paper-based microfluidic devices, Lab Chip. 16 (2016) 925–931.

[30] T. Satarpai, J. Shiowatana, A. Siripinyanond, Paper-based analytical device for sampling , on-site preconcentration and detection of ppb lead in water, Talanta. 154 (2016) 504–510.

[31] K. Huang, K. Xu, W. Zhu, L. Yang, X. Hou, C. Zheng, Hydride generation for headspace solid-phase extraction with CdTe quantum dots immobilized on paper for sensitive visual detection of selenium, Anal. Chem. 88 (2016) 789–795.

[32] B.M. Jayawardane, I.D. McKelvie, S.D. Kolev, Development of a gas-diffusion microfluidic paper-based analytical device (μPAD) for the determination of ammonia in wastewater samples, Anal. Chem. 87 (2015) 4621–4626.

[33] P. Phansi, S. Sumantakul, T. Wongpakdee, N. Fukana, N. Ratanawimarnwong, J. Sitanurak, et al., Membraneless gas-separation microfluidic paper-based analytical devices for direct quantitation of volatile and nonvolatile compounds, Anal. Chem. 88 (2016) 8749–8756.

[34] J. Nie, Y. Zhang, L. Lin, C. Zhou, S. Li, L. Zhang, et al., Low-cost fabrication of paper-based microfluidic devices by one-step plotting, Anal. Chem. 84 (2012) 6331–6335.

[35] F. Pena-Pereira, I. Lavilla, C. Bendicho, Paper-based analytical device for instrumental-free detection of thiocyanate in saliva as a biomarker of tobacco smoke exposure, Talanta. 147 (2016) 390–396.

[36] C.A. Schneider, W.S. Rasband, K.W. Eliceiri, NIH image to ImageJ: 25 years of image analysis, Nat. Methods. 9 (2012) 671–675.

[37] S. Fragueiro, I. Lavilla, C. Bendicho, Headspace sequestration of arsine onto a

Pd(II)-containing aqueous drop as a preconcentration method for electrothermal atomic absorption spectrometry, Spectrochim. Acta Part B At. Spectrosc. 59 (2004) 851–855.

[38] H.E. Emam, M.K. El-Bisi, Merely Ag nanoparticles using different cellulose fibers as removable reductant, Cellulose. 21 (2014) 4219–4230.

[39] A.A. Omrani, N. Taghavinia, Photo-induced growth of silver nanoparticles using UV sensitivity of cellulose fibers, Appl. Surf. Sci. 258 (2012) 2373–2377.

[40] M. Harada, E. Katagiri, Mechanism of silver particle formation during photoreduction using in situ time-resolved saxs analysis, Langmuir. 26 (2010) 17896–17905.

[41] C.A. Chaplan, H.T. Mitchell, A.W. Martinez, Paper-based standard addition assays, Anal. Methods. 6 (2014) 1296–1300.

[42] A. Safarzadeh-Amiri, P. Fowlie, A.I. Kazi, S. Siraj, S. Ahmed, A. Akbor, Validation of analysis of arsenic in water samples using Wagtech Digital Arsenator, Sci. Total Environ. 409 (2011) 2662–2667.

[43] N. Yogarajah, S.S.H. Tsai, Detection of trace arsenic in drinking water: challenges and opportunities for microfluidics, Environ. Sci. Water Res. Technol. 1 (2015) 426–447.

[44] S.P. Pande, L.S. Deshpande, S.N. Kaul, Laboratory and field assessment of arsenic testing field kits in Bangladesh and West Bengal, India, Environ. Monit. Assess. 68 (2001) 1–18.

[45] C.M. George, Y. Zheng, J.H. Graziano, S. Bin Rasul, Z. Hossain, J.L. Mey, et al., Evaluation of an arsenic test kit for rapid well screening in Bangladesh, Environ. Sci. Technol. 46 (2012) 11213–11219.

[46] M. Pfeiffer, G. Batbayar, J. Hofmann, K. Siegfried, D. Karthe, S. Hahn-Tomer,

Investigating arsenic (As) occurrence and sources in ground, surface, waste and drinking water in northern Mongolia, Environ. Earth Sci. 73 (2014) 649–662.

[47] M. Salman, M. Athar, W. Zaman, U. Shafique, J. Anwar, R. Rehman, et al., Micro-determination of arsenic in aqueous samples by image scanning and computational quantification, Anal. Methods. 4 (2012) 242–246.

[48] M.M. Rahman, K. Fujinaga, Y. Seike, M. Okumura, A simple in situ visual and tristimulus colorimetric method for the determination of trace arsenic in environmental water after its collection on a mercury(II)-impregnated paper, Anal. Sci. 20 (2004) 165–170.

[49] A. Baghel, B. Singh, P. Pandey, K. Sekhar, A Rapid field detection method for arsenic in drinking water, Anal. Sci. 23 (2007) 135–137.

[50] P. Nath, R.K. Arun, N. Chanda, A paper based microfluidic device for the detection of arsenic using a gold nanosensor, RSC Adv. 4 (2014) 59558–59561.

[51] Y. Zhou, X. Huang, C. Liu, R. Zhang, X. Gu, G. Guan, et al., Color-multiplexing-based fluorescent test paper: Dosage-sensitive visualization of arsenic(III) with discernable scale as low as 5 ppb, Anal. Chem. 88 (2016) 6105–6109.

[52] M. Valcárcel, Unreliability of screening methods, Anal. Chim. Acta. 516 (2004) 67–74.

[53] M. Valcárcel, S. Cárdenas, Vanguard-rearguard analytical strategies, TrAC - Trends Anal. Chem. 24 (2005) 67–74.

[54] A. D'Ulivo, Z. Mester, J. Meija, R.E. Sturgeon, Mechanism of generation of volatile hydrides of trace elements by aqueous tetrahydroborate (III). Mass spectrometric studies on reaction products and intermediates, Anal. Chem. 79 (2007) 3008–3015.

[55] J. He, T. Kunitake, A. Nakao, Facile in situ synthesis of noble metal nanoparticles in porous cellulose fibers, Chem. Mater. 15 (2003) 4401–4406.

[56] N. Wiberg, Holleman-Wiberg's Inorganic Chemistry, 34th ed., Academic Press, San Diego, 2001.

Figure captions

Figure 1. Schematic representation of the system used for *in situ* generation of the volatile derivative (through the injection zone of the paper substrate) and its subsequent chemical reaction with the recognition element present at the detection zone of the PAD.

Figure 2. Effect of the color mode detection (RGB, grayscale (GS) and MCYK) on the analytical signal. Conditions: As(III) concentration, 100 ng mL^{-1}; Paper type, Whatman No. 1; Mass of $AgNO_3$, 1 mg; $NaBH_4$ concentration, 1% (m/v); HCl concentration, 1 mol L^{-1}; Microextraction time, 10 min. Corrected mean intensities appear as squares filled with solid color, whereas blank values appear as squares filled with diagonal crossing lines.

Figure 3. Effect of the mass of $AgNO_3$ on the analytical signal. Conditions: As(III) concentration, 100 ng mL^{-1}; Whatman No. 3; $NaBH_4$ concentration, 1% (m/v); HCl concentration, 1 mol L^{-1}; Microextraction time, 10 min.

Figure 4. Effect of the arsine generation conditions on the analytical signal: Concentration of $NaBH_4$ (A), HCl (B) and ascorbic acid (C). Conditions: As(III) concentration, 100 ng mL^{-1}; Paper type, Whatman No. 3; Mass of $AgNO_3$, 1 mg; Microextraction time, 10 min.

Figure 5. Effect of microextraction time on the analytical signal. Conditions: As(III) concentration, 100 ng mL^{-1}; Paper type, Whatman No. 3; Mass of $AgNO_3$, 1 mg; $NaBH_4$ concentration, 1% (m/v); HCl concentration, 1 mol L^{-1}.

Figure 6. Plots of the mean color intensity *vs* As(III) concentration (A) and total inorganic As concentration (B). Plots of $K/[(I_{max}/I) - 1]$ *vs* As(III) concentration (C) and total inorganic As concentration (D). The detection zones of PADs exposed to increasing concentrations of arsine are shown in the inset of **Figs. 6A** and **6B**.

Figure 7. Probability-concentration graph for the screening of total inorganic As in waters with the cut-off value set at 7 ng mL^{-1}.

Figure 8. SEM images of PADs in the absence (A) and presence of AsH_3 generated from 10, 100, 200 and 400 ng mL^{-1} As (B-E). EDS spectrum of a PAD exposed to AsH_3 generated from a 400 ng mL^{-1} As solution (F).

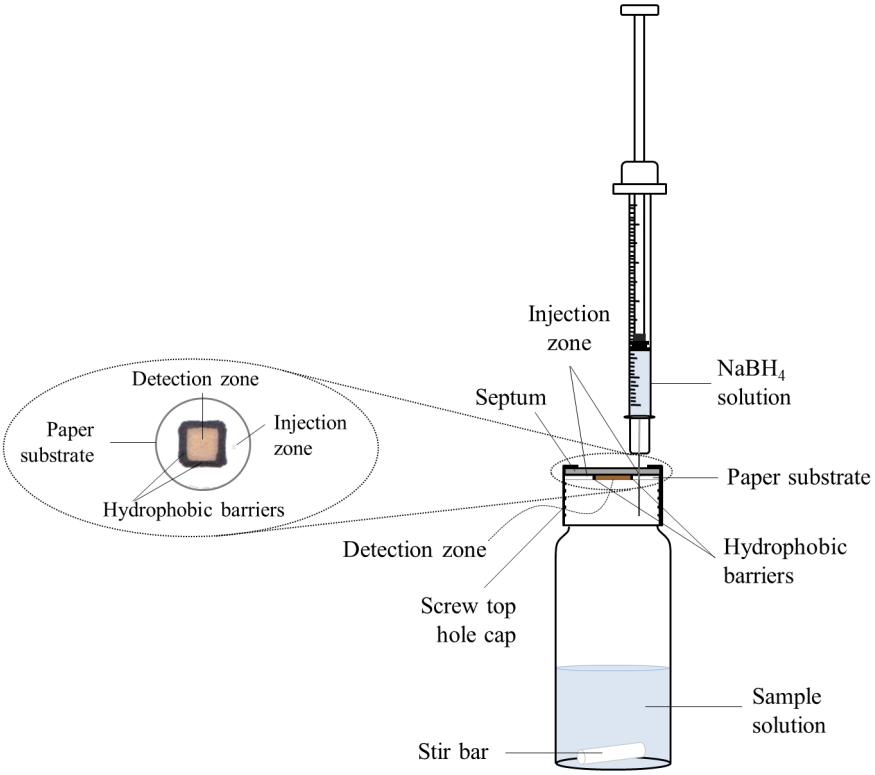
Detection zone
Paper substrate
Injection zone
Hydrophobic barriers
Injection zone
Septum
NaBH4 solution
Paper substrate
Detection zone
Hydrophobic barriers
Screw top hole cap
Sample solution
Stir bar

Figure 1

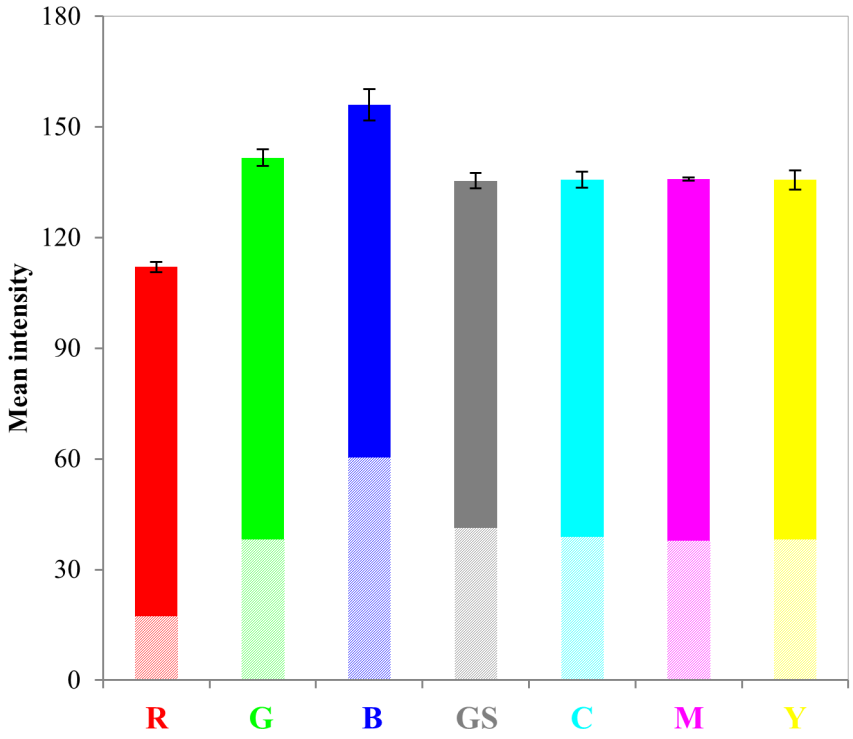

Figure 2

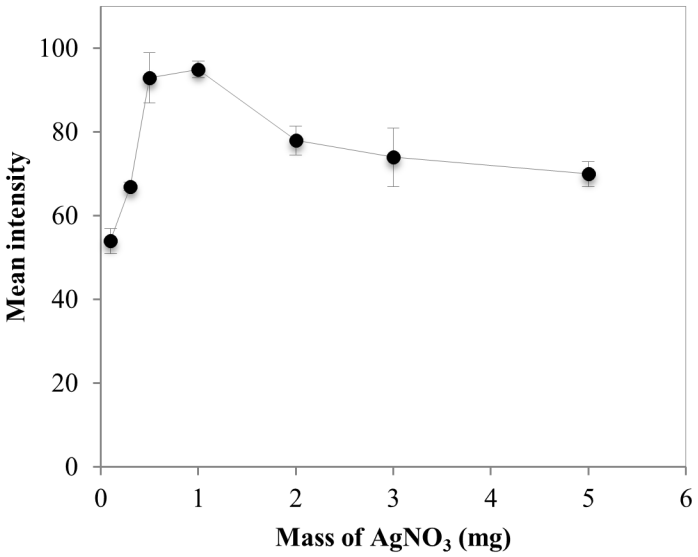

Figure 3

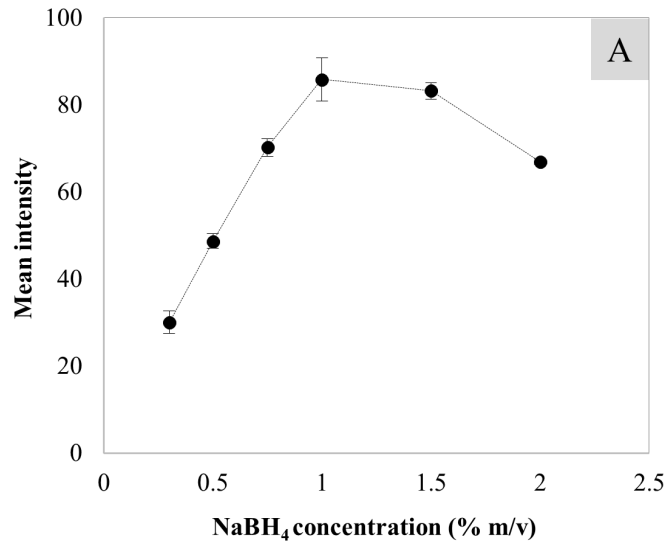
A
Mean intensity
100
80
60
40
20
0
0
0.5
1
1.5
2
2.5
NaBH4 concentration (% m/v)

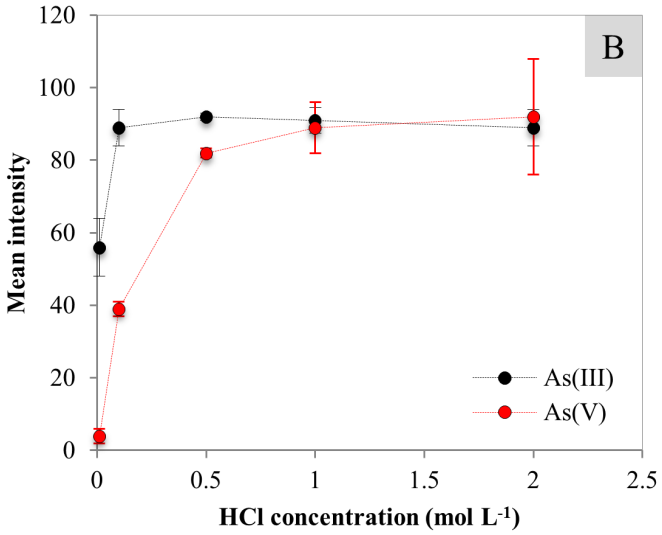
B
Mean intensity
120
100
80
60
40
20
0
0
0.5
1
1.5
2
2.5
As(III)
As(V)
HCl concentration (mol L-1)

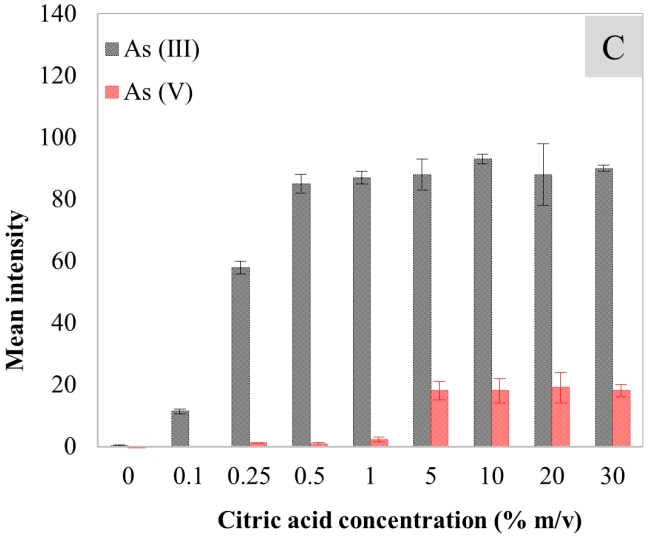
C
As (III)
As (V)
Mean intensity
140
120
100
80
60
40
20
0
0
0.1
0.25
0.5
1
5
10
20
30
Citric acid concentration (% m/v)

Figure 4

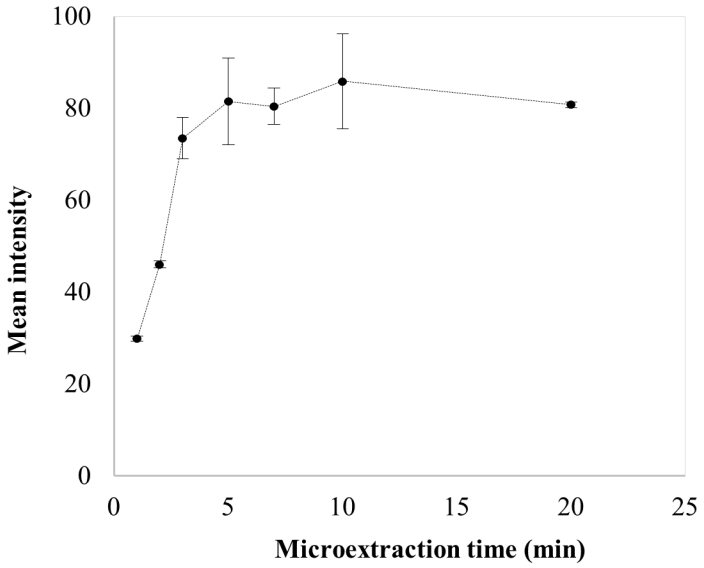
100
80
60
40
20
0
Mean intensity
0
5
10
15
20
25
Microextraction time (min)

Figure 5

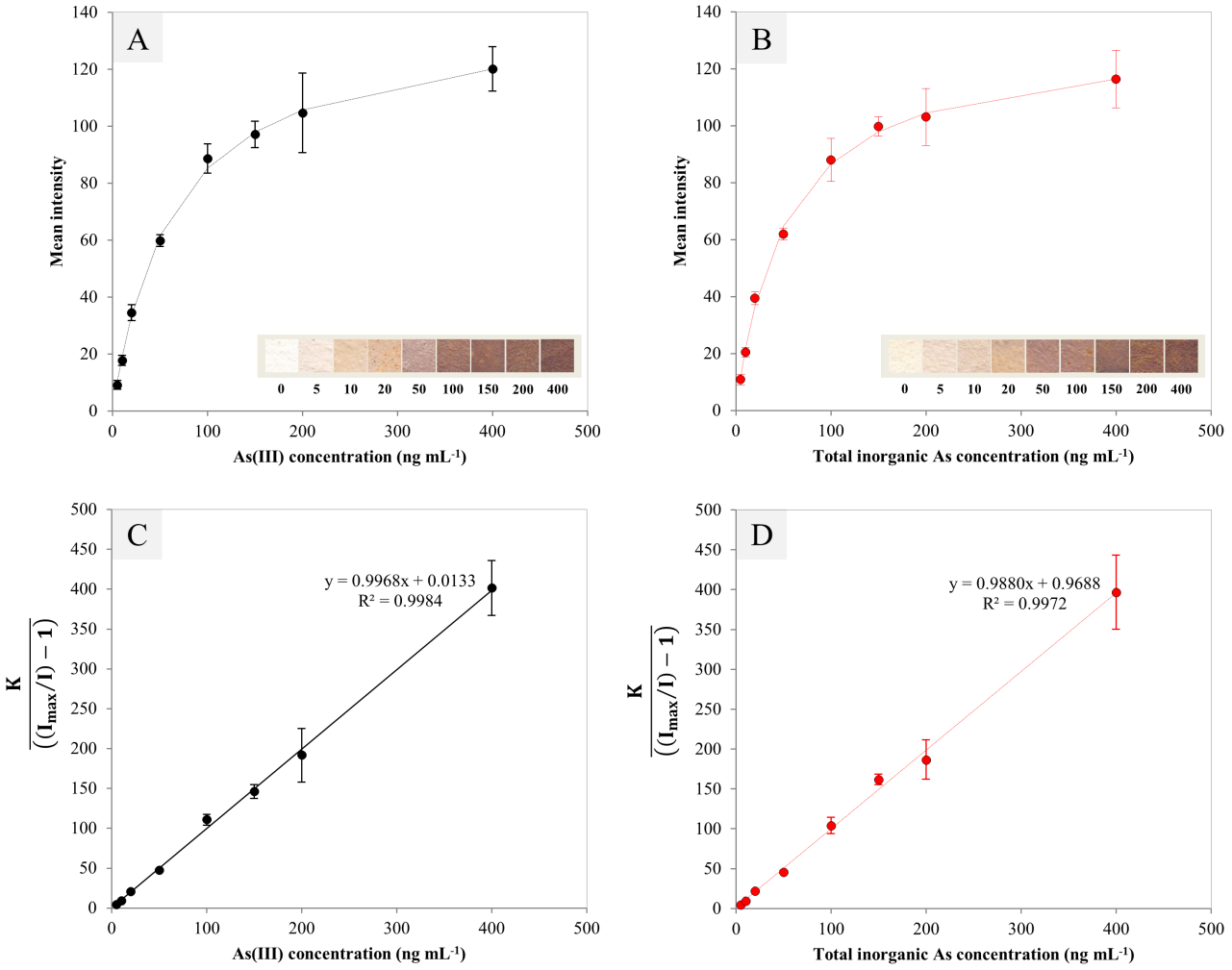
A
Mean intensity
As(III) concentration (ng mL-1)
0 5 10 20 50 100 150 200 400
B
Mean intensity
Total inorganic As concentration (ng mL-1)
0 5 10 20 50 100 150 200 400
C
y = 0.9968x + 0.0133
R² = 0.9984
K / ((Imax/I) − 1)
As(III) concentration (ng mL-1)
D
y = 0.9880x + 0.9688
R² = 0.9972
K / ((Imax/I) − 1)
Total inorganic As concentration (ng mL-1)

Figure 6

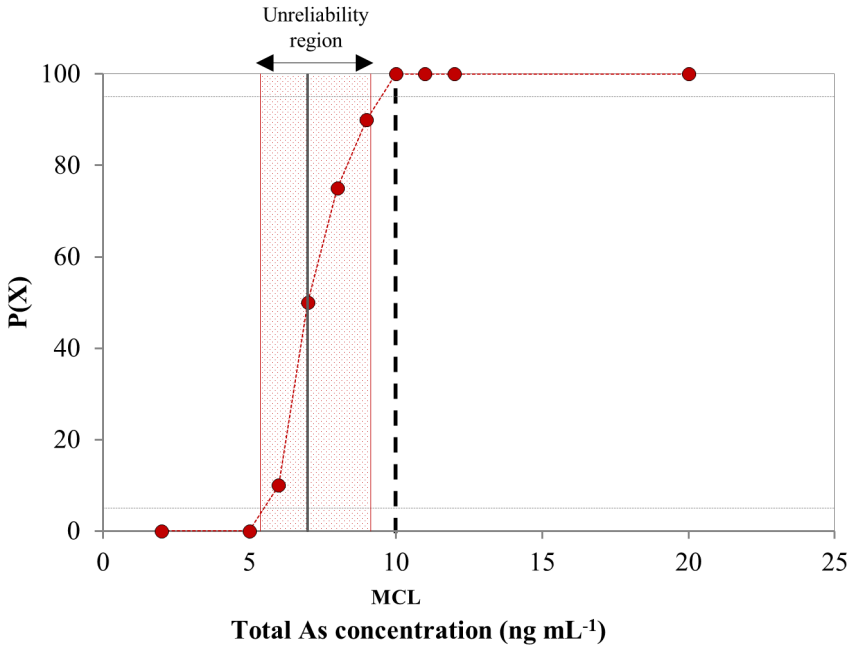
Unreliability region
100
80
60
40
20
0
P(X)
0
5
10
15
20
25
MCL
Total As concentration (ng mL-1)

Figure 7

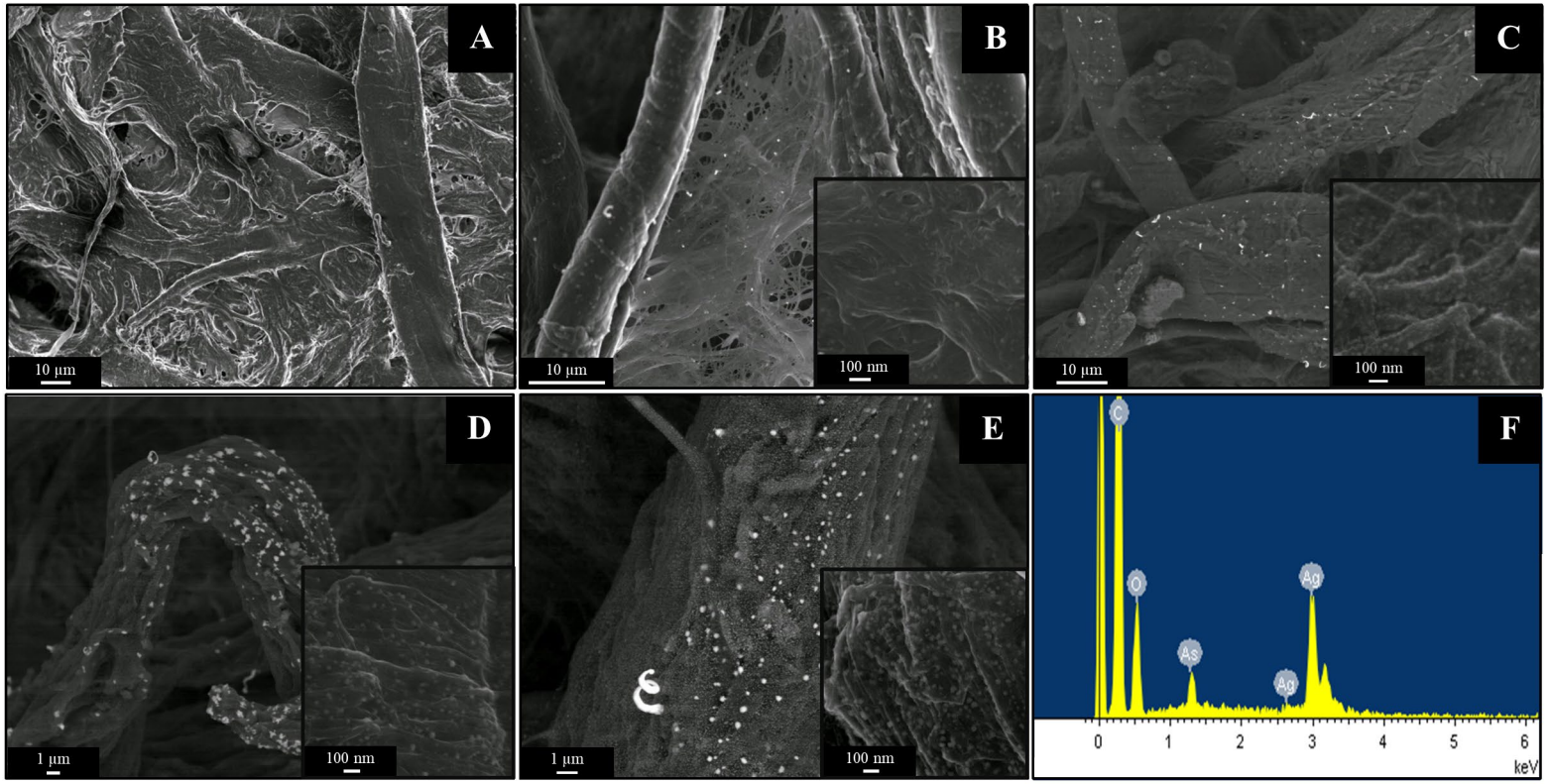
A
10 µm
B
10 µm
100 nm
C
10 µm
100 nm
D
1 µm
100 nm
E
1 µm
100 nm
F
C
O
As
Ag
Ag
0
1
2
3
4
5
6
keV

Figure 8

Table 1

Comparison of the proposed method with alternative methodologies for As determination in water samples

As species	Analytical method	Method basis	LOD (ng mL^{-1})	LDR[a] (ng mL^{-1})	Repeatability (RSD, %)	Analysis time (min)	Sample volume (mL)	Ref.
Total As	Arsenator (digital readout)	AsH_3 generation, $HgBr_2$	4.4	10-100	3.3-15.2	20	50	[42]
Total As	AAN colorimetric kit	AsH_3 generation, $HgBr_2$	20	20-700	--	30	100	[43,44]
Total As	E. Merck colorimetric kit	AsH_3 generation, $HgBr_2$	50	100-3000	--	30	100	[43,44]
Total As	NIPSOM colorimetric kit	AsH_3 generation, $HgBr_2$	20	20-700	--	5	100	[43,44]
Total As	Hach EZ colorimetric kit	AsH_3 generation, $HgBr_2$	10	10-500	--	20-40	50	[45]
Total As	ARSOlux biosensor kit	Luminescent bacterial biosensor	5	5-200	--	120	1	[46]
Total As	Colorimetric kit	AsH_3 generation, $HgBr_2$	1	2-20	1.3-5.1	5	4	[47]
Total As	Colorimetric kit	AsH_3 generation, $HgBr_2$ and rosaniline chloride	1	5-30	3.0-7.4	30	15	[48]
Total As	Colorimetric kit	AsH_3 generation, $AuCl_3$	10	--	--	10	100	[49]
As(III)[b]	μ-PAD-naked eye detection	AuNPs-TA-TG[c]	1.0	10-10000	--	5	3	[50]
As(III)	PAD-fluorimetric detection	Cyan CDs and GSH/DTT-CdTe QDs[d]	≤5	5-240	--	--	1	[51]
As(III), As(V), total As	HS-PAD-scanometric	AsH_3 generation, $AgNO_3$	1.1	5-400	7.1	5	5	This work

[a]Linear dynamic range.
[b]Other As species were not evaluated in this work.
[c]AuNPs-TA-TG, gold nanoparticles chemically conjugated with thioctic acid and thioguanine.
[d]Cyan CDs and GSH/DTT-CdTe QDs, Cyan carbon dots and Cdte quantum dots modified with gluthatione and dithiothreitol.

Table 2

Analytical results obtained by applying the proposed method to the determination of As(III), As(V) and total inorganic As in water samples

Sample	Added (ng mL^{-1})		Found (ng mL^{-1})		
	As(III)	As(V)	As(III)	As(V)	Total inorganic As
Bottled drinking water	--	--	<LOD	<LOD	<LOD
	10	--	9.6±1.8	<LOD	10.2±1.1
	10	10	10.7±0.3	10.4±1.1	21.1±1.1
Fountain water	--	--	<LOD	<LOD	<LOD
	10	--	11.15±0.04	<LOD	10.1±1.2
	10	10	9.4±0.7	10.7±2.8	20.2±2.8
River water	--	--	<LOD	<LOD	<LOD
	10	--	10.2±0.6	<LOD	9.3±0.6
	10	10	10.1±0.5	11.1±0.9	21.2±0.9
Seawater	--	--	<LOD	<LOD	<LOD
	10	--	10.4±0.3	<LOD	10.6±1.5
	10	10	9.95±0.14	9.8±1.1	19.8±1.1